Salt-Induced Universal Slowing Down of the Short-Time Self-Diffusion of a Globular Protein in Aqueous Solution

Supporting Information

Marco Grimaldo,[a,b] **Felix Roosen-Runge,**[a] **Marcus Hennig,**[a,b] **Fabio Zanini,**[b,f] **Fajun Zhang,**[b] **Michaela Zamponi,**[c,d] **Niina Jalarvo,**[c,e] **Frank Schreiber,**[b] **Tilo Seydel**[*a]

[a] *Institut Max von Laue - Paul Langevin (ILL), CS 20156, F-38042 Grenoble, France*
[b] *Institut für Angewandte Physik, Universität Tübingen, D-72076 Tübingen, Germany*
[c] *Jülich Centre for Neutron Science (JCNS), Forschungszentrum Jülich GmbH, D-52425 Jülich, Germany*
[d] *JCNS Outstation at the MLZ, Lichtenbergstraße 1, D-85747 Garching, Germany*
[e] *Chemical and Engineering Materials Division, Neutron Sciences Directorate, and JCNS Outstation at the Spallation Neutron Source (SNS), Oak Ridge National Laboratory, Oak Ridge, TN 37831, USA*
[f] *Present address: Max-Planck Institute for Developmental Biology, Spemannstraße 35, D-72076 Tübingen, Germany*
[*] *E-mail: seydel@ill.eu*

1 Amplitudes of density fluctuations

Here we discuss a hypothetical picture of cluster formation via dynamic density fluctuations. The increase of attractive interactions between proteins due to bound Y^{3+} ions on the protein surface enhances fluctuations of the local volume fraction φ and thus leads to a density distribution $G(\varphi)$. Fluctuations in φ decrease the averaged apparent self-diffusion coefficient throughout the sample, since most proteins experience a denser packing.

The average diffusion coefficient can be written as:

$$D_{\mathrm{av}} = D_0 \int_0^{\phi^{\max}} G(\varphi)\, \varphi\, \beta(\varphi)\, \mathrm{d}\varphi, \tag{1}$$

where $G(\varphi)$ is the probability density function of the local volume fraction φ, $\phi^{\max}$ is the maximum packing fraction, D_0 represents the dilute limit diffusion coefficient of a protein and $\beta(\varphi)$ is the theoretical reduced diffusion coefficient, such as that by Tokuyama and Oppenheim[1].

We could not reproduce the experimental data assuming a unimodal probability distribution of local volume fractions. However, some well-separated bimodal distributions could explain the damping of the dynamics as e.g. in the limiting case of a distribution consisting of two delta functions

$$G(\varphi) = \delta(\varphi - (\phi - A)) + \delta(\varphi - (\phi + A)) \ ,$$

corresponding to square-wave-like fluctuations with an amplitude A around the average volume fraction ϕ (cf. Figure 1).

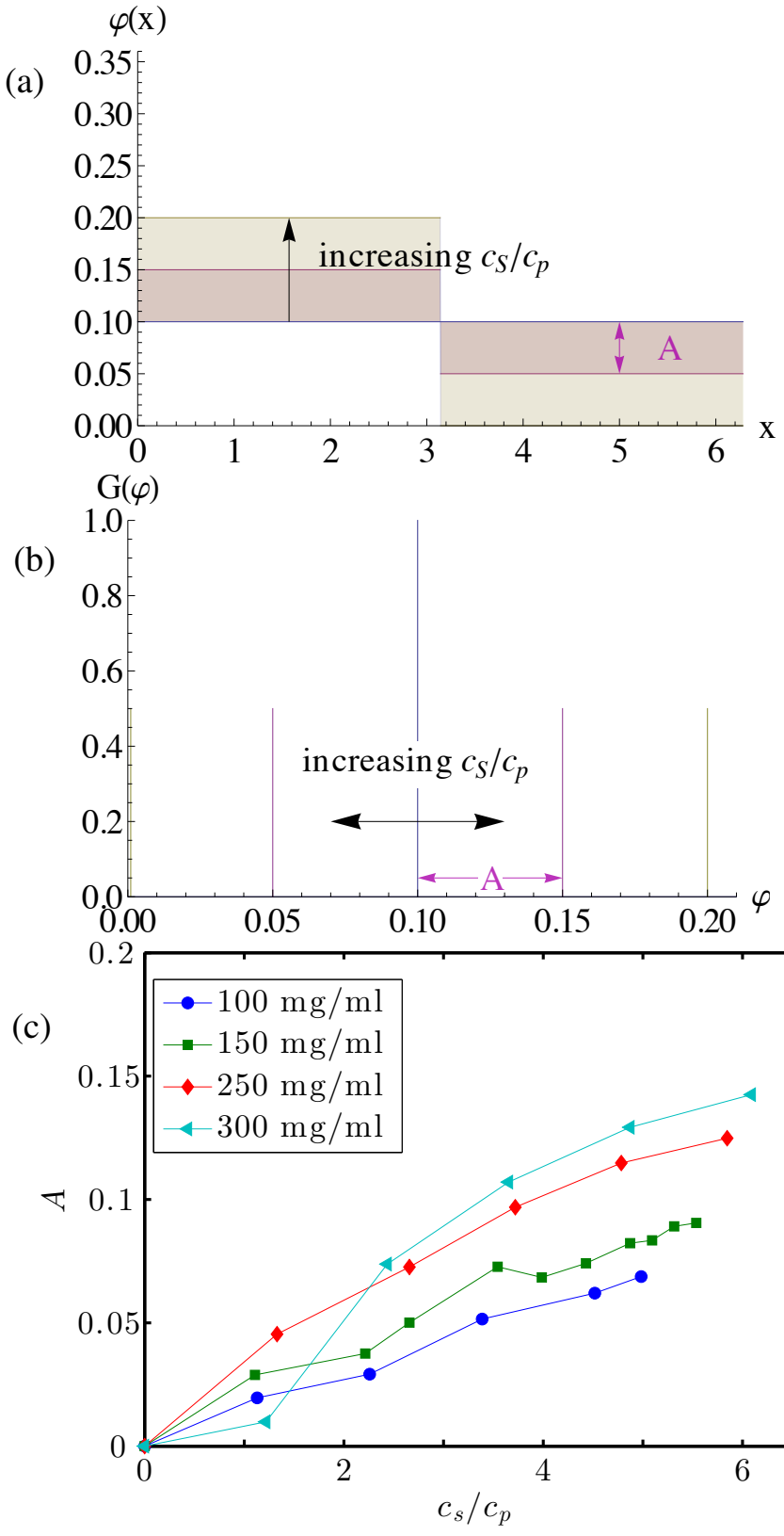

Figure 1 (a) Local density $\varphi(x)$ as a function of the position x for a square-well-like fluctuation. Increasing salt concentration c_s/c_p increases the amplitude A of the fluctuation. (b) Probability density $G(\varphi)$ of local volume fractions φ as a function of φ, in the limiting case of Delta-functions (corresponding to the spatial profile shown in (a)). With increasing c_s/c_p, $G(\varphi)$ evolves from a single peak to two peaks at distance A from the average volume fraction ϕ. (c) Amplitude A of density fluctuations as a function of c_s/c_p obtained from the fit of experimental data under the assumption of square-well-like density fluctuations.

At this point, two aspects seem difficult to reconcile with a physical explanation along this scenario: (i) There is no obvious physical reason for a well-separated bimodal distribution $G(\varphi)$ away from a phase separation. (ii) There is no obvious physical reason why density fluctuations should produce a universal scaling, since this implies a very specific relation between the fluctuation amplitude and the overall protein and salt concentration (see Figure 1(c)).

2 Subtraction of the signal of the empty sample holder with the Paalman-Pings coefficients

In order to remove from the spectra the contribution of the sample holder, the Paalman-Pings coefficients, accounting for the q-dependent absorption of neutrons by the sample and the cell walls, have beeen used[2]. The scattering intensity I^s of the sample without contribution of the empty cell is

$$I^s(\mathbf{q},\omega) = \alpha_{sc}(\mathbf{q}) I^{sc}_{sc}(\mathbf{q},\omega) - \beta_{sc}(\mathbf{q}) I^c_c(\mathbf{q},\omega) \ , \tag{2}$$

where I^{sc}_{sc} represents the scattering intensity after scattering and absorption from both the sample and the cell and I^c_c depicts the scattering intensity after scattering and absorption from the cell only. α and β are defined as follows:

$$\begin{aligned} \alpha_{sc} &= \frac{1}{A^s_{sc}} \\ \beta_{sc} &= \frac{1}{A^s_{sc}} \frac{A^c_{sc}}{A^c_c} \ . \end{aligned} \tag{3}$$

Therein $A^s_{sc}, A^c_{sc}, A^c_c$ denote the q dependent cylindrical absorption factors called Paalman-Pings coefficients. They are in turn defined as the integral

$$A^V_\Sigma(\mathbf{q}) = \frac{1}{V} \int_V \exp\left[- \int_{\gamma(\mathbf{x})} \Sigma(\mathbf{x}') \mathrm{d}s(\mathbf{x}') \right] \mathrm{d}^3\mathbf{x} \ , \tag{4}$$

where V denotes the scattering volume (either of the sample, or of the cell), γ indicates the path of a scattered neutron, $\Sigma(\mathbf{x})$ is the linear attenuation coefficient at position $\mathbf{x}$ and $\mathrm{d}s(\mathbf{x})$ depicts the infinitesimal line element of the line integral. The values of the attenuation coefficients have been calculated using the National Institute of Standards and Technology (NIST) utility[3]. The density ρ used in the calculation of the linear attenuation coefficient of the BSA solutions was obtained for a concentration $c_p = 200$mg/ml as follows:

$$\rho = (1-\varphi)\rho_{\mathrm{D_2O}} + \varphi \ \rho_{\mathrm{BSA}} \ , \tag{5}$$

where $\varphi = 0.136$ is the protein volume fraction, without hydration shell and $\rho_{\mathrm{BSA}} = 1.36\mathrm{g\ cm^{-3}}$. With $\rho_{\mathrm{D_2O}} = 1.1050\mathrm{g\ cm^{-3}}$, the density of the solution results $\rho = 1.14\mathrm{g\ cm^{-3}}$. This value has been used for the calculation of the Paalman-Pings coefficients, which were used for all the samples, since the variation in density of the investigated solutions results in variations of the linear attenuation coefficient of the order of a few percent and thus of acceptable magnitude.

3 Number density of n-clusters

Figure 2 depicts the number density ρ^*_n of the n-clusters calculated using the result for the bonding probability p_b from the main article.

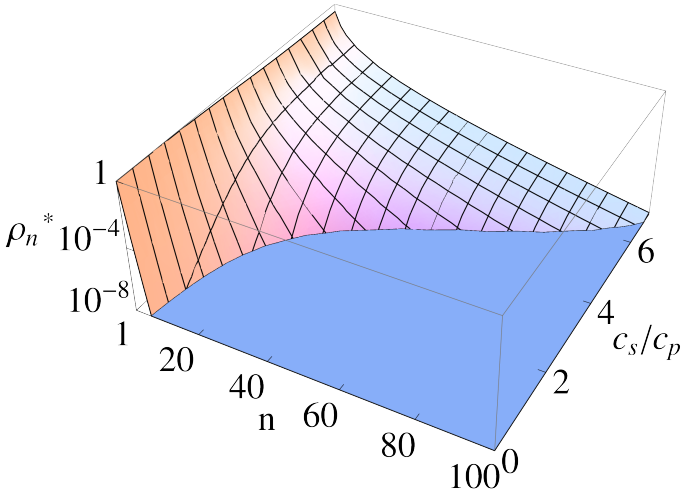

Figure 2 Number density ρ_n^* of n-clusters according to equation (3) of the main article computed using the bonding probability p_b obtained from the experiment (figure 2 of the main article), plotted versus the number n of proteins per cluster and the ratio of the salt concentration c_s and protein concentration c_p.

References

[1] M. Tokuyama and I. Oppenheim, *Phys. Rev. E*, 1994, **50**, 16–19.

[2] H. Paalman and C. Pings, *J. Appl. Phys.*, 1962, **33**, 2635–2639.

[3] NIST, *http://www.ncnr.nist.gov/resources/sldcalc.html*.